This is the author's version of an article that has been published in: *2017 IEEE Asia Pacific Microwave Conference (APMC)*, IEEE, 2017, pp. 775-778. Changes were made to this version by the publisher prior to publication.The final version of record is available at: https://doi.org/10.1109/APMC.2017.8251563

# Broadband Millimeter-Wave Detector Based on Triple-Barrier Resonant Tunneling Diode and Tailored Archimedean Spiral Antenna

Andreas Rennings [#], Benedikt Sievert [#], Wanjiao Liu [#], Khaled Arzi [*], Werner Prost [*], Daniel Erni [#]

[#] *General and Theoretical Electrical Engineering (ATE) and* [*] *Solid-State Electronics (HLT), Faculty of Engineering, University of Duisburg-Essen, D-47048 Duisburg, Germany.*
Email: andre.rennings@uni-due.de

***Abstract*—In this paper we present a millimeter-wave detector based on a triple-barrier resonant tunneling diode and a broadband Archimedean spiral antenna (ASA). Due to the conjugate matching between them, the power transfer from the receiving antenna to the rectifying diode is maximized. Besides the broadband impedance and radiation characteristics of the ASA, the circular-polarization is an essential property for mobile applications. The detector functionality has been evaluated around 200 GHz by non-linear circuit simulation, where the antenna coupling to an incoming arbitrary polarized wave is incorporated via a three-port touchstone file that has been obtained before by full-wave FEM simulation.**

***Keywords — Millimeter-wave antenna, spiral antenna, broadband antenna, resonant tunneling diode, millimeter-wave detector, non-linear modelling***

## I. INTRODUCTION

The THz-gap is still a major research challenge in high frequency engineering. Recently, silicon based RF frontends have pushed forward their figures of merit rapidly. The SiGe BiCMOS technology for example, has reached a breakthrough in providing 1 mW output power at 500 GHz [1]. Nevertheless, compound semiconductors, like GaAs, InP, or GaN are the primary choice for "real" THz-frequency, very high power, or high power–added efficiency applications using HBT [2, 3], HEMT [4], or one-terminal devices [5-7]. The resonant tunneling diode (RTD) is such a one terminal device offering a negative differential resistance (NDR) in a wide bias range. The NDR compensates resonator losses and, thus, tunneling diodes on InP with monolithically integrated antennas are offering today room-temperature fundamental-mode oscillators with the highest oscillation frequency of almost 2 THz [5].

The RTD consists of two wide band gap and ultra-thin electronic barriers. Adding another barrier forms a triple-barrier (TB) RTD. By asymmetric design of the second well these diodes provide a non-linearity in the I/V-characteristic, such that these elements are promising candidates for both, zero-bias RF signal detection [7, 8], and at positive bias, for THz oscillation [6], respectively. Therefore, the same single device can be used for both, transmission and signal detection, respectively. The detector is simply composed of the zero-biased TB-RTD, which is connected to an intrinsically broadband antenna, as been done in [7] by using a bowtie-antenna.

In this paper, we propose the spiral antenna for broadband signal detection. The tailored spiral antenna's impedance exhibits a positive reactance, whereas the input reactance of the TB-RTD is negative. By appropriate design of the antenna layout the desired conjugate match is possible, and, thus, maximal power transfer from the receiving antenna to the rectifying diode is obtained.

The paper is organized as follows. We start with section II recapitulating the resonant tunneling diode (RTD) itself, its unique features, the small signal equivalent circuit for zero-biasing, and the large signal model used for the non-linear simulation. The following section III focuses on the spiral antenna, its input impedance and the radiation characteristics. Afterwards in section IV, we demonstrate the novel combination of RTD and spiral antenna for the detector operation. Finally, in section V we give a conclusion.

## II. TRIPLE BARRIER RESONANT TUNNELING DIODE (TB RTD)

The conventional RTD is a one-terminal device consisting of several layers with optimized thicknesses and doping concentrations in order to maximize the desired effect of negative differential resistance. The current-voltage behavior exhibits basically a point symmetry (cf. Fig. 1).

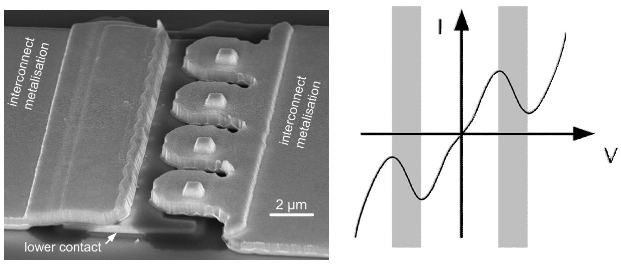


*Fig. 1.* Device layout of a four-mesa RTD with low series resistance (left) and desired current-voltage characteristic with a negative differential resistance region (right).

The triple-barrier RTD offers an extended functionality with an NDR region for the forward bias and the blocking of the reverse diode current around zero bias (cf. Fig. 2). The mentioned rectifying of the TB RTB can be utilized by a simple detector circuit composed of the antenna, the diode and a voltmeter as also sketched in Fig. 2.

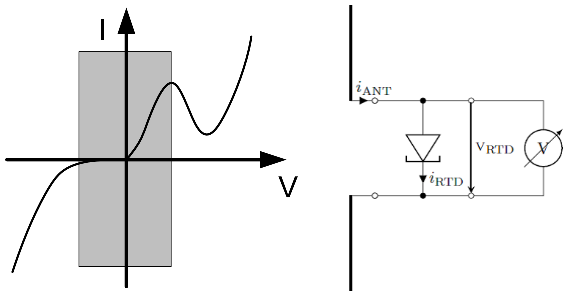


*Fig. 2.* Extended functionality of the TB-RTD shown in the idealized current-voltage diagram (left) and simple detector circuit utilizing the rectifying around zero voltage (right).

In Fig. 3 an experimental I/V-characterisitic of a TB-RTD is given [8]. The large signal behavior around zero-bias is later used for the non-linear circuit modelling in section IV.

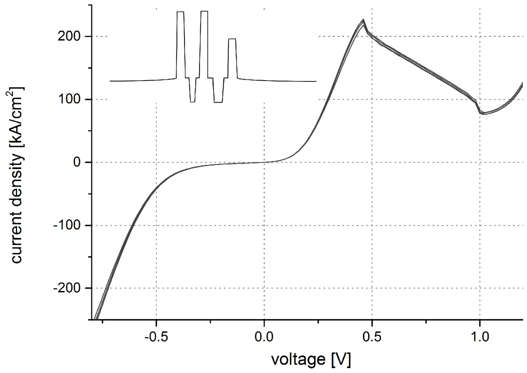


*Fig. 3.* Measured large signal behavior of the TB-RTD presented in [8].

In order to find a suitable antenna to be used in a simple detector a small-signal equivalent circuit representing the RTD for zero bias is required. Fig. 4 shows the equivalent circuit topology used here. The parameters are extracted from measured $S_{11}$ data for $V_{RTD}$ = 0 and are given within the figure.

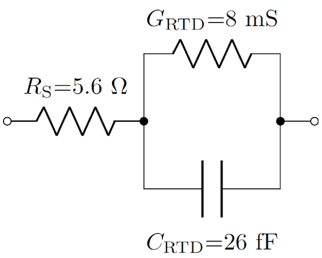


*Fig. 4.* Small-signal equivalent circuit representing the RTD for zero bias.

Due to the negative reactance of the overall RTD impedance, $Z_{\mathrm{RTD}}$, an inductive antenna impedance is required for conjugate matching. This leads us to the choice of an Archimedean spiral antenna [9].

## III. Spiral Antenna Tailored to the RTD

The Archimedian version of the spiral antenna has been chosen here, due to its broadband, smoothly varying input impedance [9]. The desired properties of the antenna structure due to the tailoring to the RTD are as follows:

- Inductive input impedance: $Z_{\mathrm{ANT}} = R_{\mathrm{ANT}} + \mathrm{j}\, X_{\mathrm{ANT}}$ with $X_{\mathrm{ANT}} > 0$
- Antenna integrable on high dielectric InP material
- Broadside beam (towards the InP side of the stack-up; the corresponding lower wave impedance causes the power flow in this direction)
- Broadband operation in terms of radiation pattern and matching

Additional antenna properties coming from the intended mobile operation of the mmw-wave detector are:

- Receiving of circular-polarized fields (high sensitivity to either left-handed (LH) or right-handed (RH) circular polarized incoming waves
- Broadside directed beam with moderate directivity (if necessary gain can be strongly increased by a lens that is attached to the InP layer)
- Good efficiency of the overall detector, thus, circuit with minimal complexity/footprint is required

A perspective view onto the Archimedean spiral antenna (ASA) is shown in Fig. 5, followed by a detailed specification of the material stack-up in Fig. 6.

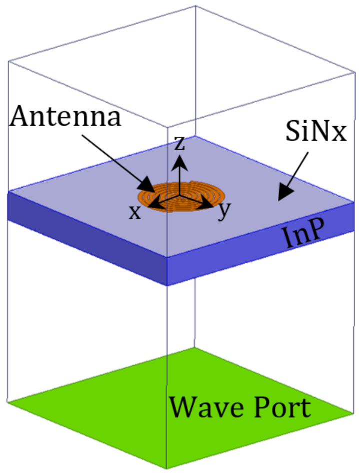


*Fig. 5.* Perspective view onto the Archimedean spiral antenna that receives circular-polarized waves excited by the indicated wave port (in HFSS).

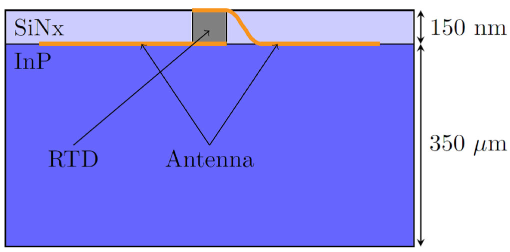


*Fig. 6.* Material stack-up consisting of an InP layer (350 µm, $\varepsilon_{r,\,\mathrm{InP}}$ = 12.5) and a SiNx layer (150 nm, $\varepsilon_{r,\,\mathrm{SiNx}}$ = 7).

As shown in the above two figures, there is no ground plane in close proximity to the spiral antenna. This is due to the balanced topology of the ASA and the corresponding balanced feeding. The ASA's metal layer is located between the thick InP and the ultra-thin SiNx layer (cf. Fig. 6). In the Finite Element Method (FEM)-based full-wave simulation with HFSS the thickness of the metal layer has been neglected. On the other hand, a finite conductivity has been considered (in HFSS, finite conductivity boundaries represent electrically thin imperfect conductors), such that, a reasonable compromise between simulation efficiency and accuracy in terms of loss modeling is achieved. The antenna's topology can be analytically formulated via, $r_{\mathrm{i}}(\alpha) = \alpha\, 20$ µm, $r_{\mathrm{o}}(\alpha) = (\alpha\, 20 + 50)$ µm, with $\alpha \in [0, 7.5\,\pi]$. The formula can be conveniently applied inside HFSS in order to carry out the FEM-based antenna design. The optimized structure of the ASA is depicted in Fig. 7. The corresponding geometrical parameters are given in the caption of Fig. 7.

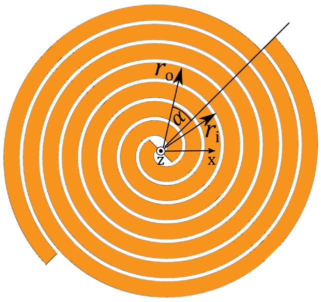


*Fig. 7.* Metal structure of the Archimedean spiral antenna with the following optimized geometrical parameters: overall diameter = 1042 µm (corresponds roughly to 0.7 $\lambda_0$ @ 200 GHz), line width = 50 µm, gap width = 13 µm.

The HFSS simulation result for the antenna impedance $Z_{\mathrm{ANT}}$ with the desired resistance and reactance behavior is depicted in Fig. 8. At least in the considered frequency range between 150 GHz up to 250 GHz the sprial antenna behaves as a "lossy inductor", and is therefore well suited to provide a conjugate match to the RTD's impedance.

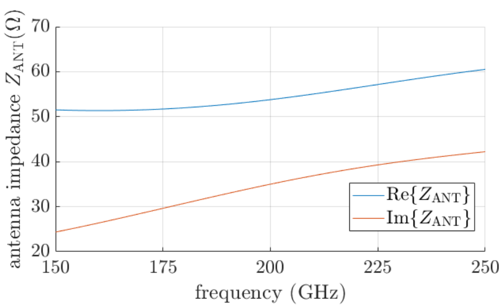


*Fig. 8.* FEM-simulated spectral response of the antenna impedance indicating a quite constant resistance and an inductive reactance well suited to conjugate match the capacitive impedance of the RTD.

The remaining antenna parameter concerns the radiation pattern. We choose a 3-D visualization in order to emphasize the nearly rotationally symmetric radiation pattern, which indicates that the detector can be arbitrarily rotated around the *z*-axis; what matters is the alignment of the broadside beam towards the incoming circular-polarized wave. In Fig. 9 the rotationally symmetric pattern for the LHCP, which is the co-polarization here, is shown for an operation frequency of 200 GHz.

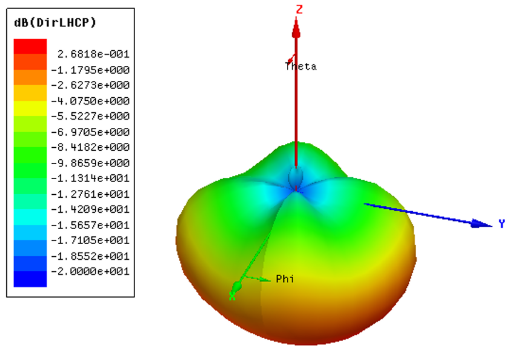


*Fig. 9.* The directivity plot for LH-circular polarization indicates a rotational symmetry, a useful property for mobile applications. The operation frequency here is 200 GHz.

The cross-polarization on the other hand, is displayed in Fig. 10. For the RHCP the main beam is in +*z*-direction with nearly the same directivity (0.3 dBi for the LHCP in –*z*-direction vs. 0.2 dBi for the RHCP in +*z*-direction). The slight difference in directivity comes from the higher permittivity of InP compared to SiNx (cf. Fig. 6), which yields an asymmetric "dielectric loading" of the spiral antenna.

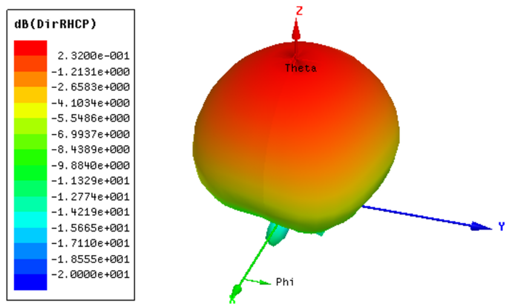


*Fig. 10.* The directivity plot for RH-circular polarization indicates again a rotational symmetry. The operation frequency here is 200 GHz, as in Fig. 9.

## IV. Detector Operation of RTD and Spiral Antenna

Here two distinct simulation types are involved, linear EM field simulation with HFSS and non-linear circuit simulation with ADS, respectively. For the HFSS simulation we consider the setup already shown in Fig. 5. A so-called wave port consisting of two "sub-ports" corresponding to *x*- and *y*-polarizations, respectively, is utilized to synthesize an incoming wave with arbitrary polarization. The polarization is controlled via the phase difference between the two sub-port signals, i.e., ±90° yields the desired LH- or RH- circular polarization. The third port in this arrangement is located in the spiral antenna's center. All three port impedances are set to the standard 50 Ω. The obtained 3x3-scattering matrix includes the coupling from the two wave ports to the antenna port. This virtual 3-port device is incorporated in the ADS circuit simulation via a touchstone file. In Fig. 11 the overall circuit in ADS is given. The two wave ports are terminated with 50 Ω loads, whereas the antenna's terminal is connected to the non-linear, large signal model of the RTD.

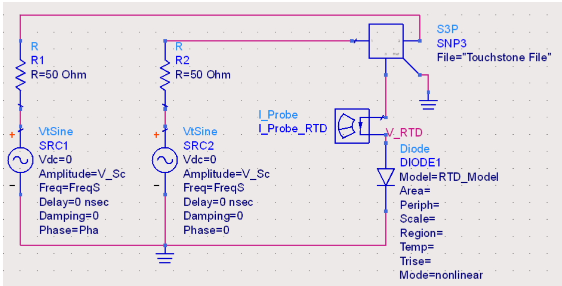


*Fig. 11.* Detector circuit in ADS: The two wave ports are excited by 50 Ω voltages sources, whereas the antenna's terminal is connected to the non-linear, large signal model of the RTD.

The first virtual experiment is carried out at 200 GHz, and the phase difference between the two wave port signals is swept over a period. Thus, we changed the polarisation of the incoming wave. In Fig. 12 the output voltage over the RTD is plotted as a function of the mentioned phase shift.

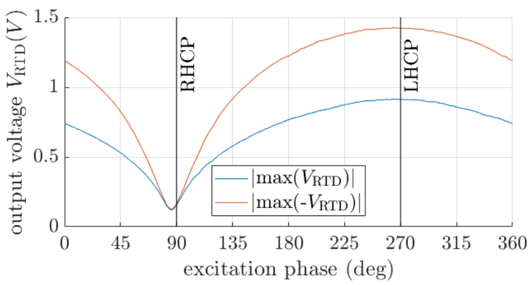


*Fig. 12.* Output voltage over the RTD (cf. Fig. 2) as a function of the polarization of the incoming wave at 200 GHz.

The plot indicates the sensitivity to the polarisation. A field with LHCP is detected with max. sensitivity, whereas the detector is quite insensitive to a RHCP, the X-polarization.. Furthermore, the rectifying of the RTD yields a larger value $|V_{RTD}|$ for a reverse current, then for the forward direction.

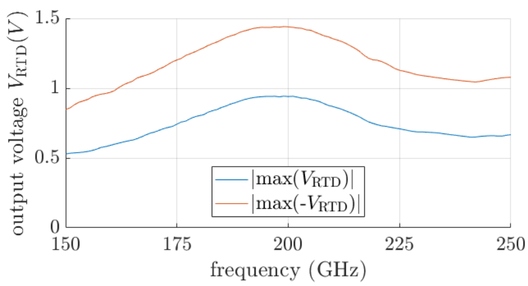


*Fig. 13.* Frequency-selective output voltage over the RTD for an LHCP incoming wave.

Finally, in the second experiment, the mentioned voltages for a LHCP as a function of frequency are plotted in Fig. 13. Here, the relatively flat responds indicates the broadband operation of the proposed detector.

## V. Conclusion and Outlook

In this work we proposed the loading of a broadband Archimedean spiral antenna with a non-linear triple-barrier resonant tunneling diode for the purpose of millimeter-wave detection. Such a detector features minimal complexity. Via full-wave EM and non-linear circuit simulation we showed the general working principle and corresponding performance.

In the near future we will fabricate the proposed detector circuit and characterize it.

## Acknowledgement

This work is partly funded by the Deutsche Forschungsgemeinschaft (DFG) within the Collaborative Research Center TRR SFB 196 MARIE and by the ITN network TeraApps of European Union within Horizon 2020.

## References


[1] U. R. Pfeiffer, Y. Zhao, J. Grzyb, R. Al Hadi, N. Sarmah, W. Förster, H. Rücker, and B. Heinemann "A 0.53 THz reconfigurable source module with up to 1 mW radiated power for diffuse illumination in terahertz imaging applications", *IEEE J. Solid-State Circuits*, vol. 49, no. 12, pp. 2938-2950, Dec. 2014. doi: 10.1109/JSSC.2014.2358570

[2] M. Seo, M. Urteaga, J. Hacker, A. Young, Z. Griffith, V. Jain, R. Pierson, P. Rowell, A. Skalare, A.. Peralta, R. Lin, D. Pukala, and M. Rodwell; "InP HBT IC technology for terahertz frequencies: fundamental oscillators up to 0.57 THz", *IEEE J. Solid-State Circuits*, vol. 46, no. 10, pp.2203, Oct. 2011.

[3] J. C. Rode, H-W Chiang, P. Choudhary, V. Jain, B. J. Thibeault, W. J. Mitchell, M. J. W. Rodwell, M. Urteaga, D. Loubychev, A. Snyder, Y. Wu, J. M. Fastenau, and A. W. K. Liu "Indium phosphide heterobipolar transistor technology beyond 1-THz bandwidth", *IEEE Trans. Electron Dev.*, vol. 62, no. 9, pp.2779, 2015.

[4] K. M. K. H. Leong, X. Mei, W. Yoshida, P-H Liu, Z. Zhou, M. Lange, L-S Lee, J. G. Padilla, A. Zamora, B. S. Gorospe, K. Nguyen, and W. R. Deal; "A 0.85 THz low noise amplifier using InP HEMT transistors", *IEEE Microwave and Wireless Comp. Lett.*, vol. 25, no. 6, pp. 397, 2015.

[5] T. Maekawa, H. Kanaya, S. Suzuki, M. Asada; "Oscillation up to 1.92 THz in resonant tunneling diode by reduced conduction loss", *Appl. Phys. Express* 9:024101, 2016.

[6] R. Sekiguchi, Y. Koyama, and T. Ouchi, „Subterahertz oscillations from triple-barrier resonant tunneling diodes with integrated patch antennas", *Applied Phys. Lett.*, 96(6), 2010.

[7] M. Suhara *et al.*, "Analysis of terahertz zero bias detectors by using a triple-barrier resonant tunneling diode integrated with a self-complementary bow-tie antenna," *70th Device Research Conference*, University Park, TX, pp. 77-78, 2012.

[8] G. Keller, A. Tchegho, B. Münstermann, W. Prost, and F-J Tegude; Characterization and modeling of zero bias detection diodes based on triple barrier resonant tunneling structures; *Int. Conf. Indium Phosphide and Related Materials*, Kobe, Japan, May 19 - 23, 2013.

[9] J. Kaiser, "The Archimedean two-wire spiral antenna", *IRE Transactions on Antennas and Propagation,* vol. 8, no. 3, pp. 312 - 323, May 1960.

**DOI:** 10.1109/APMC.2017.8251563
**URN:** urn:nbn:de:hbz:465-20221121-140801-8